

SEDIMENT TRANSPORT RATE DUE TO WAVE ACTION

By

Masaki Sawamoto
 Associate Professor, Department of Civil Engineering
 Tohoku University, Sendai 980, Japan

and

Toshihiko Yamashita
 Associate Professor, Department of Civil Engineering
 Hokkaido University, Sapporo 060, Japan

SYNOPSIS

Two formulas of sediment transport rate due to wave action are proposed. One is for the region of saltation and the other is for the sheet-flow motion. The former formula is derived by theoretical consideration in which stochastic characteristics of sand particles on the bed are taken account of. A good agreement between the experiments and the theory is confirmed. In order to derive the latter one, a series of experiments was carried out in a U-shape tube. The 1.5 power relationship of transport rate and bottom shear stress is empirically concluded for the sheet-flow motion. The limit of application of both formulas is also discussed in the paper.

INTRODUCTION

Sand drift phenomena on beaches are classified into two categories. One is that in longshore direction and the other in on-offshore one. Sediment transport rate formula of the former has been established and utilized in the numerical simulation of shoreline change. The reason why it gives good results is that the scale of phenomena concerned is some kilometers in length and some years in time. In other words, the applicability of formula in such a case can be verified through field observations or protosize test of jetties, since our interest is focussed on a long term trend. On the other hand, though some formulas have been proposed, we need more studies for the latter in which the phenomena of shorter time and smaller length scales are important.

Recently, the formula given by Madsen and Grant[9] has been often referred to estimate the on-offshore transport rate. Adopting a quasi-steady assumption, they applied the Einstein-Brown formula to an oscillatory flow field. The coefficients in the formula were determined by using the experimental data of Manohar[10], Kalkanis[5] and Abou-Seida[1]. This result describes the outline of experimental data covered in wide range. However, the third power relationship between transport rate and bed shear stress which they concluded seems not reasonable and it has been reported that their formula gives too much transport rate in certain cases[14].

It is well known that there are three types of motion of sediment under wave action; (i) saltation over a flat beds which occurs just beyond the critical shear, (ii) combined motion of saltation and suspension over rippled beds under the moderate bed shear stress, and (iii) sheet flow motion under the high bed shear flow. However, existing theories of sediment transport ignore these differences and try to represent phenomena by a single formula over a wide range.

The purpose of this paper is to derive on-offshore sediment transport

formulas for two different types of sediment movement. One is for the range of saltation and the other for sheet flow motion. In order to derive the former, Einstein's stochastic approach[2] is adopted in the theory in which the transport rate is calculated as the product of pick-up rate and step length. The latter is derived through a series of experiments in an U-shape tube which enable to generate high bed shear stress in the laboratory. The limit of application of both formulas is also discussed.

MODELING OF SALTATION AND SEDIMENT TRANSPORT RATE FORMULA

In this section, we consider a case that a *small amount of sand* moves in saltation over a flat bed under the shear stress a little bit greater than the threshold, where a *small amount of sand* means physically the amount of sand in a single surface layer of bed.

Generally speaking, the sand transport phenomena in a wave field is more complicated than in an unidirectional flow because it is a dynamic process in an unsteady flow. However, some aspects of phenomena are more easily treated in the analysis than that of steady flow if we observe it from the view point of the scale of sediment particles. It is due to the following reasons. Although the pick up rate and step length in a steady flow are strongly controlled by the turbulence, those in the wave field primarily depend on the time variation of flow associated to wave action near the bed. A sediment particle leaves bed at accelerating phase, keeps its motion during phase of high velocity and settles onto bed in decelerating phase. Therefore the threshold of motion is directly determined by the properties of sediment particle and the fluid dynamic force due to wave induced flow, and an excursion length of particle, step length, may closely relate to the integration of orbital motion of fluid particles. This fact makes us possible to discuss the mechanism by using the reliable parameters and also denies any quasi-steady approach, in which the sand transport rate is directly related to the instantaneous velocity.

In the model described here, we try to derive the sediment transport rate formula by simulating reasonably the principal processes of sand particle movement. The procedure of calculation is shown in Fig.1. At first, we calculate the bed shear stress and fluid dynamic force exerting on a particle. Taking account of the probabilistic feature of sediment, the time variation of pick up rate is evaluated. The step length of sediment is calculated by analyzing the equation of motion of sediment particle. Finally, by combining them, the transport rate of sediment is obtained.

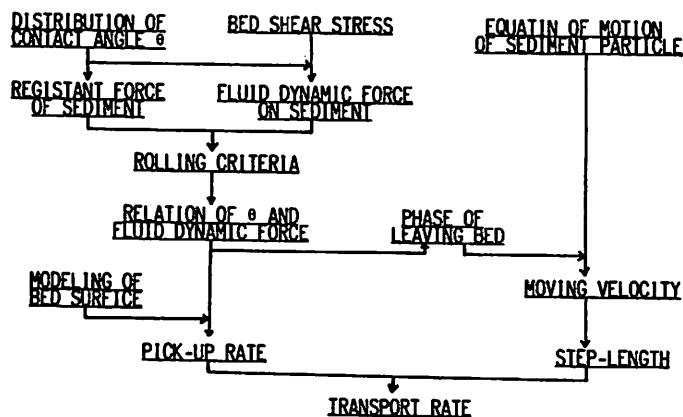


Fig.1 Procedure of calculations

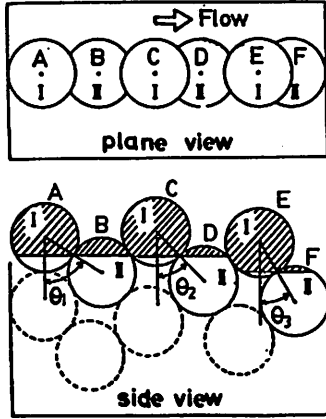
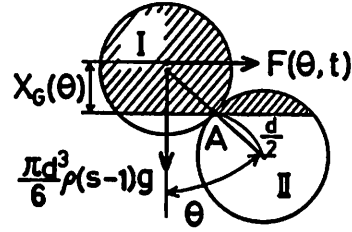


Fig.2 Arrangement of sediment particles

Fig.3
Criteria of sediment movement

Transport rate formula based on particle movement analysis

Let's consider the bed where N particles of sand with uniform diameter d are on an unit area as shown by I and II in Fig.2. The number of particles which can move firstly in a surface layer is a half of N as shown by I in the figure. If we denote a pick-up rate and step-length by $P(t)$ and $\ell(t)$ which are functions of time t , averaged sand transport rate q over a half wave period is given by

$$q = \frac{2}{T} k_3 \frac{\pi d^3}{6} \frac{N}{2} \int_0^{T/2} \ell(t) \cdot P(t) dt \quad (1)$$

where T = wave period; and k_3 = coefficient representing particle form and is unity when particles are uniform spheres.

Probability of sediment movement

The initiation of sand movement is modeled by a rolling criterion as shown in Fig.3. A particle contacting with neighbouring one by an angle θ initiates its motion when the driving moment of fluid dynamic force M_f exceeds the resisting moment by the submerged weight M_g . M_f and M_g are written as

$$M_f(\theta, t) = F(\theta, t) X_g(\theta) \quad (2)$$

$$M_g(\theta) = \rho g(s-1) \frac{\pi d^3}{6} \frac{d}{2} \sin \theta \quad (3)$$

where $F(\theta, t)$ = fluid dynamic force; $X_g(\theta)$ = arm length of $F(\theta, t)$; s = specific gravity of sediment; and ρ = fluid density.

The value of contacting angle θ is not constant as shown schematically in the figure but varies in a certain range. So we treat it as a probabilistic variable of the probability $G(\theta)$ or the density $g(\theta)$. It enable us to evaluate stochastically the resistance and fluid dynamic force of each particle. In other words, we consider the particle with small value of θ as a easily moved one because not only its resisting force is small but also it relatively juts out into the flow and suffers large fluid dynamic force and vice versa. By using the distribution of θ , the number N is represented as

$$N = k_2 \left(\frac{1}{d} \frac{k_1}{d} \right) \quad (4)$$

$$k_1 = 1 / \int_0^{90^\circ} \sin \theta \cdot g(\theta) d\theta$$

where the value of k_1 is calculated as 1.364 by using the function $g(\theta)$, which is given later part of this paper, and a constant k_2 representing an arrangement of particles and is unity under a usual condition.

There are two ways to evaluate the fluid dynamic force. One is basing on Morison's type equation and the other is to be calculated from bed shear stress. The latter is used in the model because it is better in order to discuss the relationship between the transport rate and the bed shear. The bed shear stress τ is calculated from Jonsson's friction factor f_w [3] and the diagram of f_w given by Kamphuis [6]. It is assumed that the bed shear is shared by particles in proportion to the area hatched in Fig.3 and also assumed that the arm length X_g is equal to the distance of its centroid. From these assumptions the fluid dynamic force $F(\theta, t)$ and the arm length $X_g(\theta)$ are evaluated as eqs.(5) and (6).

$$\left. \begin{aligned} F(\theta, t) &= \tau(t) S_I(\theta) / \frac{N}{2} \frac{\pi d^2}{4} \\ S_I(\theta) &= \frac{1}{4} d^2 \left(\pi - \theta + \frac{1}{2} \sin 2\theta \right) \\ \tau(t) &= \rho f_w \{ U_m \sin (2\pi t/T + \sigma) \}^2 / 2 \end{aligned} \right\} \quad (5)$$

$$X_g(\theta) = \frac{d \left[\frac{1}{8} \cos \theta \left\{ \sin(\cos \theta) + \frac{\pi}{2} \right\} + \frac{1}{8} \sin \theta - \frac{1}{24} \sin^3 \theta \right]}{\frac{1}{4} \left(\pi - \theta + \frac{1}{2} \sin 2\theta \right)} \quad (6)$$

where U_m = amplitude of wave induced flow near bed; σ = phase difference of flow and bed shear stress; and $S_I(\theta)$ = the hatched area. The probability $G(\theta)$ plays an important role in the model. This function was obtained through the experiments shown in Fig.4. The sand bed was simulated by the fixed bed with sand roughness. Some dyed sand particles were arbitrarily placed on it. Increasing the bed slope, the number of particles which start moving and the then angle, which is equivalent to the contacting angle θ , were observed. The results are shown in Fig.5. The open circles are the measured angle and the solid line is an approximated curve by the beta distribution of eq.(7).

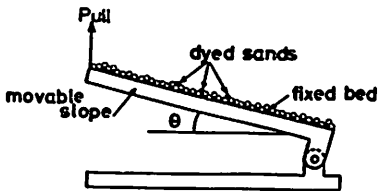


Fig.4
Measurement of contact angle θ

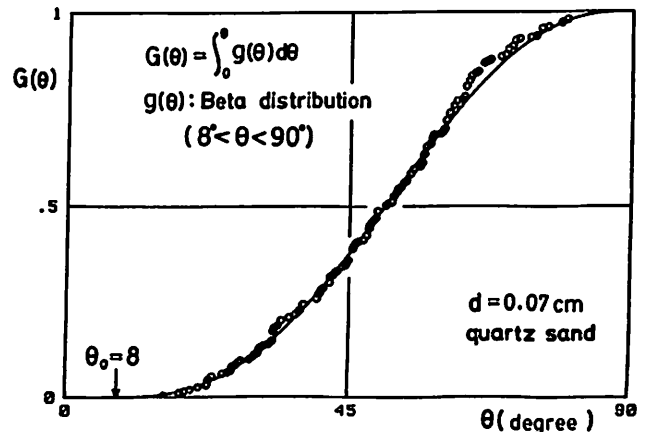


Fig.5
Probability distribution of contact angle θ

$$g(\theta) = dG(\theta)/d\theta$$

$$= \frac{(\theta - \theta_0)^{a-1} (90 - \theta)^{b-1}}{(\theta_0)^{a+b-1}} = \frac{1}{\int_0^1 \alpha^{a-1} (1 - \alpha)^{b-1} d\alpha} \quad (7)$$

where the constants $a = 3.11$, $b = 2.88$ and θ_0 is 8° . The value of k_1 mentioned before is calculated from this function.

It should be noticed that the angle obtained here is not the so-called angle of repose but the contacting one of sand particles. The relation of this angle and Shields' criteria is considered here. Since extreme angle such as $\theta = 0$ can not exist on a natural sand, there exists a certain minimum angle θ_{min} . The sand particle with θ_{min} starts moving at first under the critical condition. The angle corresponding to Shields' criterion, say $\psi_c = 0.05$, is calculated to be 8° . This value is reasonable because it agrees with a rising point of the beta distribution of θ as shown in the figure. This value is used in the eq.(7) as the lower limit θ_0 .

The procedure for the calculation of pick-up rate is as follows. At time t of accelerating phase, a critical value of θ , say $\theta_c(t)$, is obtained from eqs. (2), (3) and (5). Because the particles of which θ is smaller than $\theta_c(t)$ have already left bed, the probability $G(\theta_c(t))$ is the rate of moving particles. Therefore, the rate of particles which leave bed, pick-up rate $P(t)$, is calculated from the time derivative of $G(\theta_c(t))$.

$$P(t) = \frac{dG(\theta_c(t))}{dt} \quad (8)$$

The comparison of calculation and experiments is shown in Fig.6. In the figure, the white histogram shows the experimentally observed number of particles which leave bed and the hatched one that of settled particles onto bed. The dotted line shows the result by using of Kamphuis' diagram [6] in which the phase difference σ is ignored. The chain line is the modified one in which the effect of σ is taken account of through Kajiura's model [4]. The agreement of the latter is fairly good. The settling phase P_s calculated by the analysis mentioned below is also shown in the figure. Its agreement with the experiments is not so good.

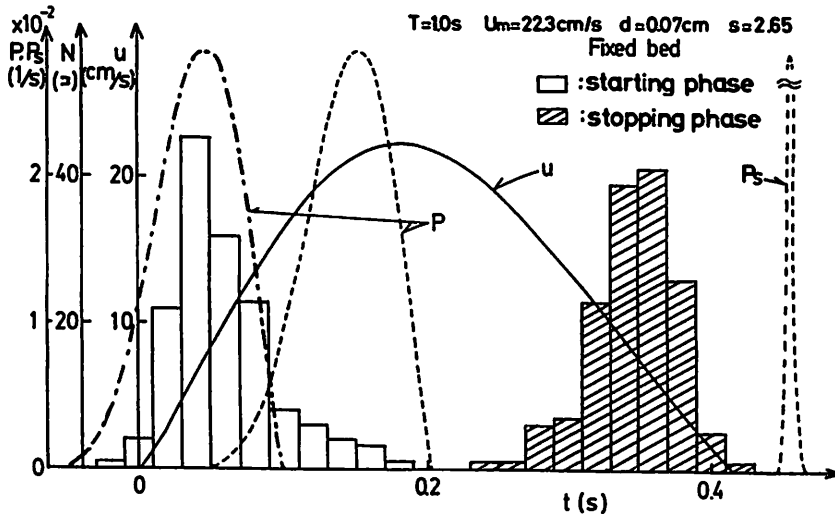


Fig.6 Pick-up rate of sediment particle

Step-length of sediment particle

The step-length is obtained by analyzing of an equation of motion of a particle. The step-length $l(t_0)$ of the particle which leaves bed at time t_0 is defined by its excursion distance at the phase when the particle velocity is zero as shown in eq.(9) .

$$\left. \begin{aligned} X_{t_0}(t) &= \int_{t=t_0}^{t=t} U_p(t_0, t) dt + X_{t_0}(t_0) \\ l(t_0) &= X_{t_0}(t \text{ when } U_p=0) - X_{t_0}(t_0) \end{aligned} \right\} \quad (9)$$

where $U_p(t_0, t)$ = velocity of particle which left bed at time t_0 and is obtained by the numerical integration of eq.(10) .

$$\frac{d U_p}{d t} = A_1 \left| U(X_{t_0}, t) - U_p(t_0, t) \right| \{ U(X_{t_0}, t) - U_p(t_0, t) \} + A_2 \frac{d U(X_{t_0}, t)}{d t} \quad (10)$$

$$A_1 = 3 C_D / 4 d (s + C_m), \quad A_2 = (1 + C_m) / (s + C_m)$$

where C_D = drag coefficient; and C_m = added mass coefficient. In eq.(10), the Basset term and another decelerating effects are neglected. The wave induced velocity was used as fluid velocity $U(x, t)$ and the influence of boundary layer was ignored in the calculation. Figs.7 and 8 show examples of analysis of sediment movement and step-length in on-shore direction. The theory predicts about 10 % larger value than the experiments. This is due to above mentioned assumptions and leads some error in transport rate formula. However, this error is much less than the scattering of experimental data and does not cause any serious problem.

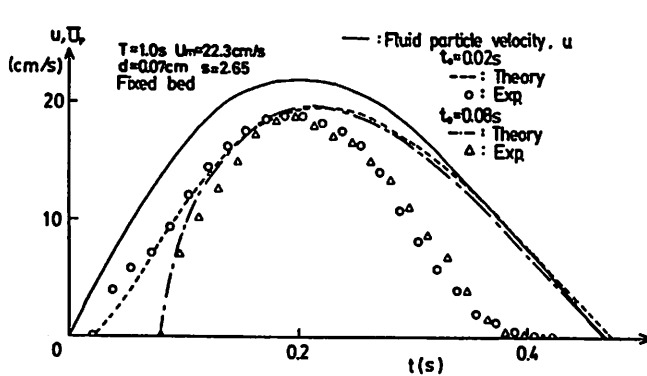


Fig.7 Motion of sediment particles

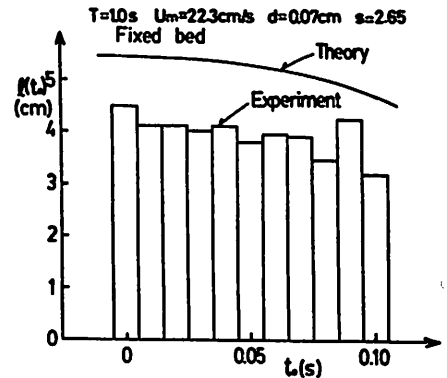


Fig.8 Step-lengths of sediment particles

Sediment transport rate

The sand transport rate evaluated by the present theory is shown in Fig.9. The abscissa is the Shields number defined by $\psi_m = \tau_m / \rho(s-1)gd$ where τ_m is an amplitude of bed shear stress. The ordinate is nondimensional transport rate $\phi = q/wd$ where w is settling velocity of sand particle in water. The experimental data [1,5], exclusive of those in sheet flow regime, and the formula given by Madsen and Grant [9] are also shown in the figure for comparison. The agreement with experiments is good except Kalkanis' data. The theory predicts

almost the same value as the Madsen and Grant formula. The discrepancy with Kalkanis' data is due to the difference of the critical Shields number used. The value of ψ_c is 0.05 in the model and it is not so unreasonable. On the other hand, Kalkanis reported the data of ψ_m less than 0.05. This fact seems to be the difference of the characteristics of experiments. In the high ψ_m range, the slope of theoretical curves becomes mild. This is due to the assumption of the model that only particles in surface layer can move. But, this region is out of range of applicability of the present theory because a formula for sheet flow motion should be applied when the multi layers of particle move.

Since the calculation is so complicated, we try to put above mentioned procedure into single explicit formula. Eq.(1) may be rewritten by using of mean pick-up rate P_0 and mean step-length ℓ_0 as

$$q = K \frac{d}{T} \ell_0 P_0 \quad (11)$$

where

$$K = \pi k_1 k_2 k_3 / 6$$

$$P_0 = \int_0^{T/2} P(t) dt \quad (12)$$

$$\ell_0 = \int_0^{T/2} \ell(t) P(t) dt / P_0$$

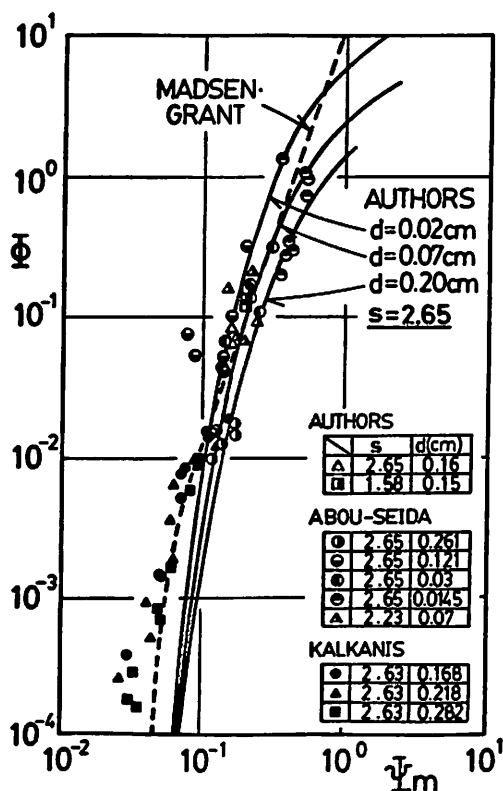


Fig.9 Comparison of theoretical model with experiments

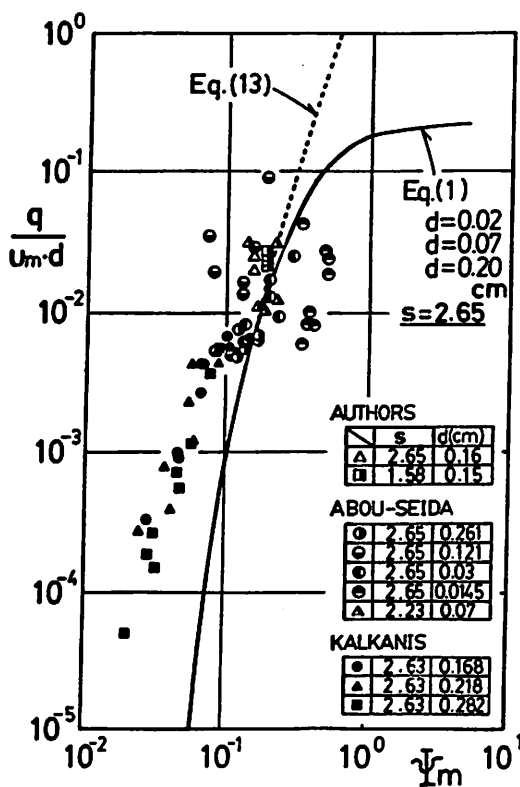


Fig.10 Comparison of simplified formula with experiments

If we write the contact angle θ of a particle which moves under the maximum bed shear τ_m as θ_{max} , P_0 is equal to $G(\theta_{max})$. We can calculate θ_{max} from eq.(5) by putting τ_m instead of τ and finally can conclude that P_0 is a function of $(\psi_m - \psi_c)$. It was confirmed through a series of trial calculations that this function may be satisfactorily approximated by

$$P_0 = 18.8 (\psi_m - \psi_c)^{2.72}$$

It was also confirmed that the step-length can be approximated by

$$\lambda_0 = 0.258 U_m T (\psi_m - \psi_c)^{0.37}$$

Rounding the index into single figure, we can conclude eq.(13) for the saltation motion.

$$q/U_m d = 5.8 (\psi_m - \psi_c)^3 \quad (13)$$

The comparison with eq.(13) and the exact calculation of eq.(1) is shown in Fig.10. The agreement of the approximate form is good in moderate range of ψ_m . It is also noticed that the results of exact calculation may be expressed by an unified curve if we use the parameters of this figure.

EXPERIMENTS OF SHEET-FLOW MOTION AND SEDIMENT TRANSPORT FORMULA

Although the condition for initiation of sheet-flow motion has been made clear [7], the sufficient data are not available in order to discuss the mechanism and transport rate, because the number of available experiments in sheet-flow regime has been limited [1,8]. Therefore we conducted a series of experiments listed in the attached tables (Table 1 and 2) at first. In order to get high bed shear stress condition, the experiments were carried out in a U-shape tube shown in Fig.11. The experimental conditions were selected by using Kaneko's regime diagram[7]. Basing on the results of experiments, an empirical formula is proposed in this section.

Observation of the sheet-flow motion

The results of observation through 16 mm movie camera for sediment # 5 and Case No.4 are shown in Fig.12(a)-(d). U_p and V_p are horizontal and vertical velocity of particles, respectively. C_p and C_{ps} are the concentration of sediment at moving and at rest on bed. The origin of y is the top of sediment layer at rest. The followings were observed.

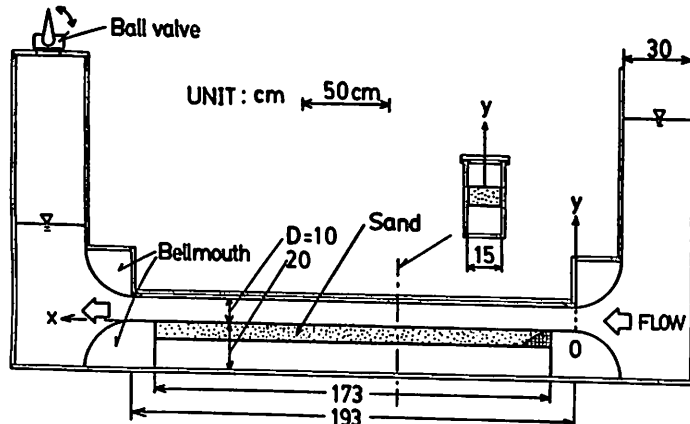


Fig.11 Schematic view of the U-shape tube

i) Particles move only one step in a half wave period and no particle moves after settling onto bed in the same half period.

ii) V_p tends to be positive in accelerating phase and negative in decelerating phase. This fact is a reflection of the development of moving layer in accelerating phase and the settlement of particles in decelerating phase. However, its value varies in a wide range and frequent collisions of particles associated violent vertical momentum transfer are guessed in the moving layer. U_p of the most upper particle is the same order of fluid velocity. But small phase lag is appreciable because of the inertia difference of sediment and fluid.

iii) Since the pressure gradient is maximum at zero velocity phase and it penetrates into the layer, particles in the deep layer are also under the easily movable at this phase.

iv) The particles of upper layer suffer the fluid dynamic force and that of collision. On the other hand, the lower particles bear the forces due to pressure gradient.

The observed thickness of moving layer is shown in Fig.13. δ_m is the thickness at moving and δ_s that at rest on bed. Ψ_m is calculated from Jonsson's f_w where particle diameter d is taken as roughness k_s . We notice the linear relationship of δ_s and Ψ_m on the log-log diagram. The same relationship also noticed between δ_m and Ψ_m except the data of the most fine sand. It was observed that the suspension is relatively more dominant than the others in case of the most fine sand. Except those data, the ratio of δ_m and δ_s which is a mean concentration of moving layer is almost constant.

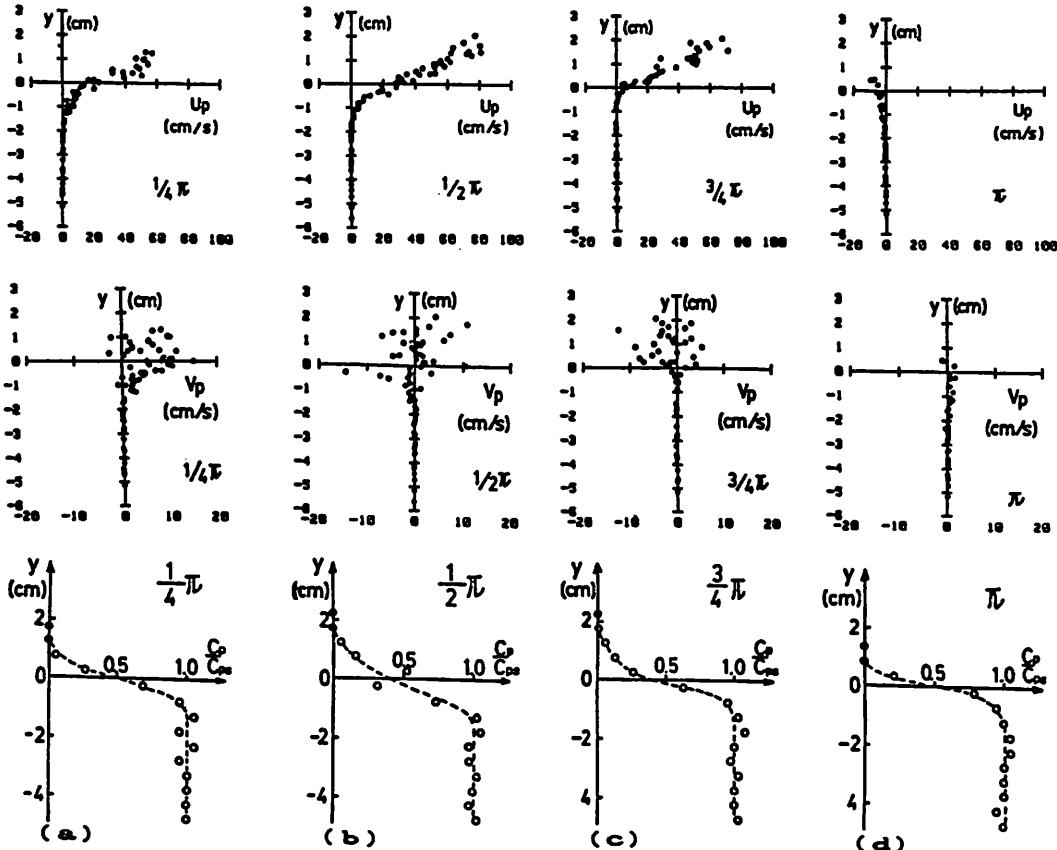


Fig.12 Distributions of U_p, V_p and C_p/C_{ps}

(a) $2\pi t/T = \pi/4$, (b) $\pi/2$, (c) $3\pi/4$ and (d) π .

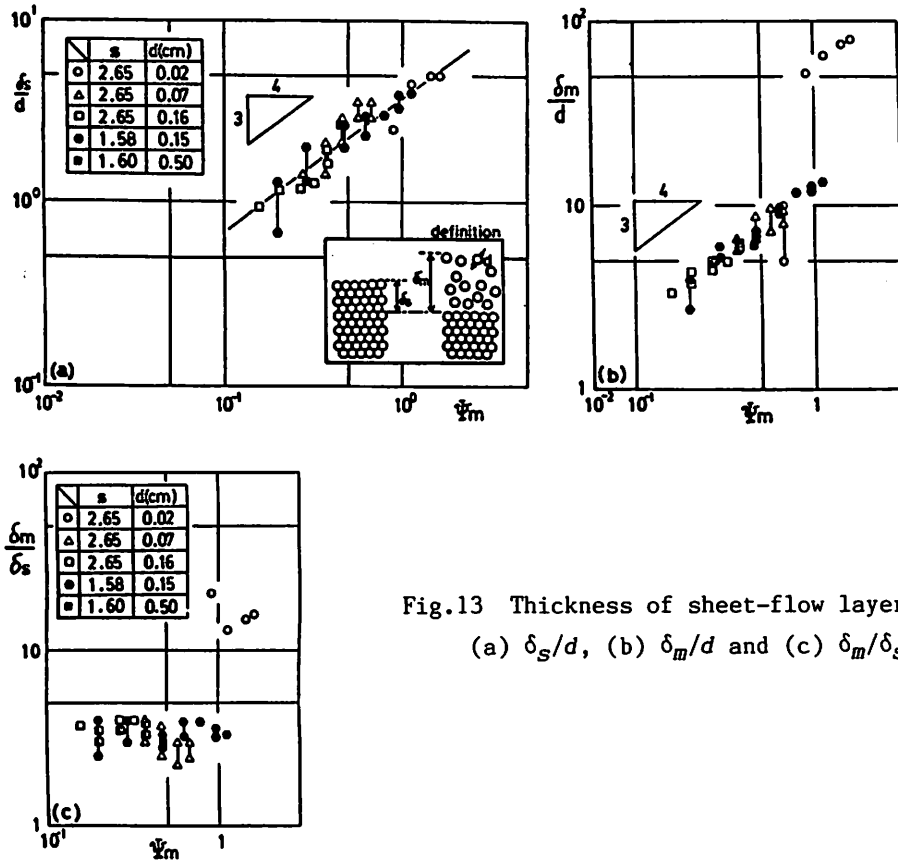


Fig.13 Thickness of sheet-flow layer
(a) δ_s/d , (b) δ_m/d and (c) δ_m/δ_s

Sediment transport rate

Fig.14 shows the data of transport rate by the authors and others [1,8]. The only data in sheet-flow regime are shown in the figure. The conventional parameters are used. The Madsen and Grant formula [9] is also shown for comparison. It is easily noticed that their formula explains the outline of data covering wide range of ψ_m . But we also notice that the particles with same diameter are on different lines. In other words, the data suggest show the 1.5 power relationship of ϕ and ψ_m for each particle with different diameter, though the Madsen and Grant formula represents the third power relationship. This is a reason that their formula may give too much transport rate under the circumstance of large ψ_m .

It is an important problem what power relationship between the transport rate and bed shear stress we conclude. Another problem is what kinds of nondimensional parameters are reasonable. The former is related to whether the formula properly represents the mechanism, and the latter does whether all physical properties related are taken account of. Here we tried a dimensional analysis. All nondimensional parameters possible were examined. The best result obtained by this way is shown in Fig.15. The solid line is represented by eq.(14).

$$\phi = 2.2 \left(U_{*m} / w \right)^3 \quad (14)$$

where the shear velocity U_{*m} is defined by

$$U_{*m} = \sqrt{\tau_m / \rho}$$

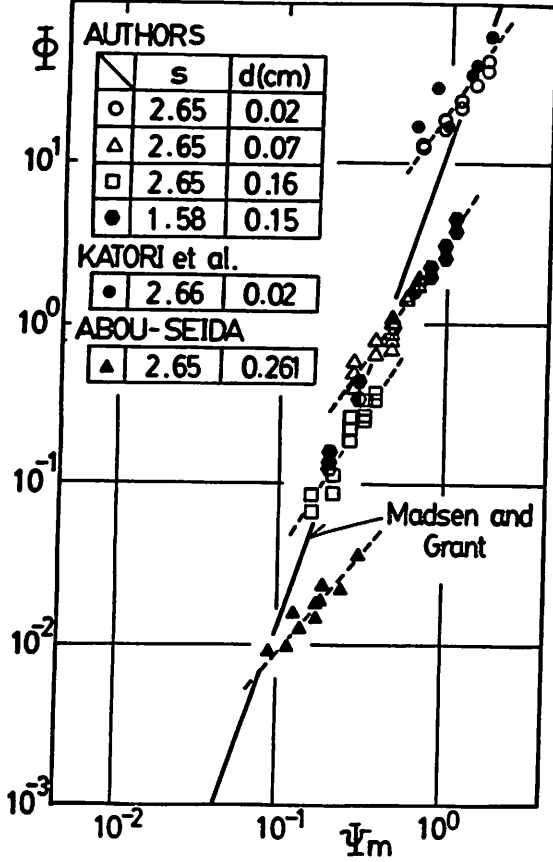


Fig.14 Sediment transport rate
(ϕ versus ψ_m)

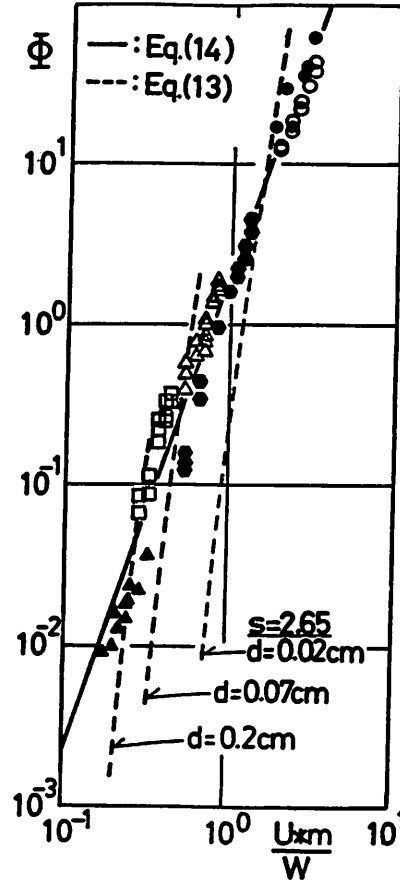


Fig.15 Sediment transport rate
(ϕ versus U_{*m}/W)

This equation may be rewritten into following form.

$$\phi = 2.2 \left(\frac{\sqrt{(s-1)gd}}{w} \right)^3 \psi_m^{1.5} \quad (15)$$

Fig.14 suggests that ϕ is proportional to the 1.5 power of ψ_m and that its proportional constant is a function of the sediment property. In eq.(15), this function is represented by the minus third power of nondimensional settling velocity. In other words, eq.(15) is an improved form where the effect of the settling velocity is more properly included. Therefore, we propose eq.(14) or (15) as the sediment transport rate formula in sheet-flow regime.

CONSIDERATIONS

We should notice that eq.(13) and eq.(14) are written by using different parameters each other. This comes from the fact that the mechanism of sediment transport is quite different in each regime. Therefore, if we plotted the data of sheet-flow regime on Fig.10, they would scatter. In case that we plot the saltation data on Fig.15, the situation is the same.

Let's consider the limit of application of eqs.(13) and (14). If we conducted the experiments over flat bed and increased the bed shear, saltation would be observed at first stage where eq.(13) is applicable. As bed shear stress increased, the phenomena would change into the sheet-flow motion in which eq.(14) applies. Therefore we obtain transition limit from eq.(13) to eq.(14) by equating the transport rate of both equation. The result is eq.(16).

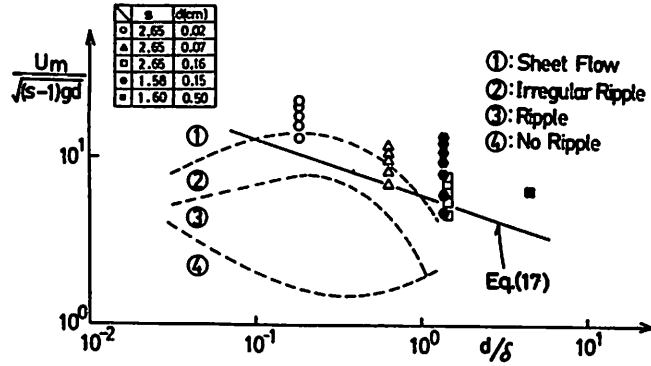


Fig.16 Regime of sediment transport type

$$U_m/w = 1.97 \psi_m^{-1.5} \quad (16)$$

Fig.16 shows the comparison of eq.(16) and Kaneko's criterion obtained through experiments[7]. Since the parameters used in the figure and eq.(16) are different, the values of each parameter were calculated separately for given sediments and experimental conditions. Eq.(16) falls on the solid line which is approximated by eq.(17) .

$$U_m/\sqrt{(s-1)gd} = 6.0 (d/\delta)^{-1/3}, \quad \delta = \sqrt{\nu T/\pi} \quad (17)$$

The upper broken curve is a limit of sheet-flow motion and irregular ripple obtained by his observation. Eq.(17) corresponds to this limit in a large d/δ range. The discrepancy is appreciable in the range of small d/δ where viscous effect is dominant. But eq.(16) or (17) is still useful because the sand transport due to wave action occurs in the range of larger d/δ .

Although we have propose sediment tranport formula over a half wave period, net transport rate over a wave period is more important in the calculation of shore process. In the present study, the net sediment transport results from two kinds of mechanism. One is the effect of progressive wave, just like the Stokes drift, and the other is due to the asymmetry variation of bed shear in onshore and offshore direction. The former is automatically taken into account of in the analysis of step-length. The latter would be evaluated if the asymmetry of velocity variation is given by an appropriate theory. Some trial calculations have shown that the latter is more important in ordinary circumstances.

Under the condition where sand ripples are generated, the results obtained here are concerned in matters in two ways. The authors[11] reported the procedure for the estimation of suspended sediment concentration over rippled beds. The formula for saltation would improve this calculation. Eq.(13) leads to the transport rate proportional to the third power of shear stress for rippled beds like as Shibayama [13]. But, the direction of transport over ripples is so complicated that it is still difficult to derive the unified formula for rippled beds.

The model of saltation presented here is also applicable to explain the ripple generation. Since the model includes not only the final transport rate but also the mechanism of sediment movement, it is easily applied to the phenomenon of nonequilibrium sediment transport which is essential to the instability of sand beds. This process has been reported by the authors[13].

ACKNOWLEDGMENTS

The authors wish to thank to Mr. Yoshinobu Akiyama, Taisuke Yamazaki and Hiromi Yokoyama, for their collaboration in the experimental works. The support

of the grant of the Department of Civil Engineering, Tokyo Institute of Technology, is also appreciated.

Table-1 Characteristics of the sediments

sediment #	material	specific gravity s	diameter d (mm)	settling velocity w (cm/s)
# 1	quartz sand A	2.65	0.2	2.50
# 2	quartz sand B	2.65	0.7	10.5
# 3	quartz sand C	2.65	1.8	22.5
# 4	coal dust	1.58	1.5	7.60
# 5	imitation pearl	1.60	5.0	25.1

Table-2 Experimental conditions

Case No.	period T (s)	amplitude of velocity U_m (cm/s)
1	3.8	125.3
2	3.8	114.6
3	3.8	101.5
4	3.8	88.7
5	3.8	74.4
6	3.8	56.2
7	3.8	44.3
8	3.12	80.6

Table-3 Sediment transport rate

sediment #	case No.	transport-rate q (cm ² /s)	sediment #	case No.	transport-rate q (cm ² /s)
#-1	1	1.92	#-3	1	1.17
		2.22			1.31
		1.90			1.18
#-1	2	1.58	#-3	2	0.942
		1.57			0.881
		1.24			0.917
#-1	3	1.12	#-3	3	0.659
		0.819			0.784
		0.940			0.313
#-1	5	0.629	#-3	4	0.405
		0.654			0.233
					0.302
#-2	1	1.29	#-4	1	5.17
		1.42			4.33
		1.23			2.94
		1.27			3.53
		1.27			2.55
#-2	2	1.37	#-4	3	2.26
		1.03			1.85
		1.08			1.82
		1.08			1.07
		0.567			1.09
#-2	3	0.498	#-4	5	0.497
		0.624			0.385
		0.733			0.179
		0.783			0.154
		0.572			0.140
#-2	4	0.466	#-4	7	
		0.461			
		0.283			
		0.421			
		0.356			

REFERENCES

1. Abou Seida, M.M. : Bed load function due to wave action, Univ. of California Berkeley, Hydraulic Engineering Lab. Rep. HEL-2-11, 1965.
2. Einstein, H.A. : The bed-load function for sediment transportation in open channel flows, U.S. Dept. of Agric., Soil Conservation Service, Tech. Bull. No.1026, 1950.
3. Jonsson, I.G. : Wave boundary layer and friction factors, Proc. of 10th Int. Conf. on Coastal Eng., pp.127-148, 1966.
4. Kajiura, K. : A model of the bottom boundary layer in water waves, Bull. of Earthq. Res. Inst. Univ. of Tokyo, Vol.46, pp.75-123, 1968.
5. Kalkanis, G. : Transportation of bed material due to wave action, U.S. Army, Corps of Engineers, CERC, Tech. Memo. No.2, 1964.
6. Kamphuis, J.W. : Friction factor under oscillatory waves, Proc. of ASCE, WW2, pp.135-144, 1975.
7. Kaneko, A. : A study of sand ripples generated under oscillatory flow, thesis dissertation, Kyushu Univ., 1981.
8. Katori, S., A. Watanabe and K. Horikawa : Laboratory study on sediment movement in the sheet flow regime, Proc. of 27th Japanese Conf. on Coastal Eng., pp.202-206, 1980 (in Japanese).
9. Madsen, O.S. and W.D. Grant : Sediment transport in the coastal environment, Rep. No.209, Ralph M. Parsons Laboratory, M.I.T., 1976.
10. Manohar, M. : Mechanics of bottom sediment movement due to wave action, U.S. Army, Corps of Engineers, Beach Erosion Board, Tech. Memo. No.75, 1955.
11. Sawamoto, M. and S. Yamaguchi : Theoretical Modeling on wave entrainment of sand particles from rippled beds, Proc. of JSCE, No.288, pp.107-113, 1979 (in Japanese).
12. Sawamoto M., T. Yamashita and Y. Akiyama : Stability theory of sand ripples due to wave, Proc. of 31st Japanese Conf. on Coastal Eng., pp.376-380, 1984 (in Japanese).
13. Shibayama, T. : Laboratory study on sediment transport mechanism due to wave action, Proc. of JSCE, No.296, pp.131-141.
14. Vincent, C.E., R.A. Young and D.J.P. Swift : Bed-load transport under waves and currents, Marine Geology, 39, pp.71-80.

APPENDIX - NOTATION

The following symbols are used in this paper:

- a, b = coefficients of Beta distribution;
 A_1, A_2 = coefficients in equation of motion for sediment particle;
 C_D, C_m = drag and added mass coefficients;
 C_p, C_{ps} = concentration of sediment at moving and at rest;
 d = diameter of sediment particle;
 F = fluid dynamic force on sediment;
 f_w = Jonsson's friction factor;
 g = acceleration of gravity;
 $g(\theta)$ = probability density of θ ;
 $G(\theta)$ = probability of θ ;
 k_1, k_3 = coefficients representing particle form;
 k_2 = coefficient representing particle arrangement;
 K = $\pi k_1 k_2 k_3 / 6$;
 ℓ = step length of sediment particle;

λ_0	= mean step length;
M_f	= driving moment of fluid dynamic force;
M_g	= resisting moment of sediment by the submerged weight;
N	= number of sediment on an unit area;
P	= pick up rate of sediment particle;
P_0	= mean pick up rate;
q	= sediment transport rate;
s	= specific gravity of sediment;
t	= time;
T	= wave period;
U	= velocity of fluid;
U_m	= amplitude of U ;
U_{*m}	= shear velocity defined by τ_m ;
U_p	= horizontal velocity of sediment particle;
V_p	= vertical velocity of sediment particle;
w	= settling velocity of sediment in water;
X_g	= arm length of F ;
X_{t0}	= position of sediment which leaves bed at t_0 ;
δ	= Stokes layer thickness;
δ_m	= thickness of moving layer;
δ_s	= settled thickness of moving layer;
θ	= contact angle of sediment;
θ_0	= lower limit of θ ;
θ_c	= critical value of θ for given bed shear stress;
ρ	= density of water;
σ	= phase difference between shear stress and velocity;
τ	= bed shear stress;
τ_m	= maximum bed shear stress;
ϕ	= nondimensional sediment transport rate;
ψ_m	= Shields parameter defined by maximum shear stress; and
ψ_c	= critical Shields parameter.